Fluid Mechanics
2015; 1(2): 5-10
Published online August 31, 2015 (http://www.sciencepublishinggroup.com/j/fm)
doi: 10.11648/j.fm.20150102.11

PIV Study of the Turbulent Flow in a Stirred Vessel Equipped by an Eight Concave Blades Turbine

Bilel Ben Amira, Zied Driss, Mohamed Salah Abid

Laboratory of Electromechanical Systems (LASEM), National School of Engineers of Sfax (ENIS), University of Sfax (US), Sfax, Tunisia

Email address:
bba.amira7@gmail.com (B. B. Amira), Zied.Driss@enis.tn (Z. Driss), MohamedSalah.Abid@enis.rnu.tn (M. S. Abid)

To cite this article:
Bilel Ben Amira, Zied Driss, Mohamed Salah Abid. PIV Study of the Turbulent Flow in a Stirred Vessel Equipped by an Eight Concave Blades Turbine. *Fluid Mechanics*. Vol. 1, No. 2, 2015, pp. 5-10. doi: 10.11648/j.fm.20150102.11

Abstract: The purpose of this study is to experimental investigating of the hydrodynamics structure in a cylindrical stirred vessel generated by an eight concave blades turbine. Particle image velocimetry (PIV) system was used to evaluate the effect of the blade turbine in the flow fields. The flow is illuminated by a Nd: YAG 532 nm green pulsed laser source generated in 2x30 mJ. The acquisition of the tow-dimensional images data was taken with a CCD camera with 1600 x 1200 pixels² of resolutions. In addition, a mini-synchronizer was used to control the different PIV components. For the results, we are interested to present the distribution of the velocity fields, the vorticity, the turbulent kinetic energy, the dissipation rate of the turbulent kinetic energy and the turbulent viscosity. Three azimuthally planes were carried out which present the turbine blade plane (θ=30°), the upstream turbine blade plane (θ=10°) and the downstream turbine blade plane (θ=45°).

Keywords: PIV, Flow, Stirred Vessel, Concave Blades, Turbine

1. Introduction

Stirred tanks are widely used in the industrial applications. In fact, several experimental and numerical studies have been carried out in the literature. For example, Driss et al. [1] studied the hydrodynamic structure induced by double helical ribbons and double helical screw ribbons impellers. Chtourou et al. [2] compared four turbulence models in a cylindrical tank occupied with a Rushton turbine. Subsequently, Bouzgarrou et al. [3] studied the hydrodynamic structure of three helice types. Driss et al. [4] studied the flow generated within a retreated-blade paddle and a flat-blade paddle. Karray et al. [5] investigated the interaction between the flow and the impeller structure in order to calculate the displacement of the anchor blade. Xuereb and Bertrand [6] used Computational Fluid Dynamics (CFD) to analyze the fields of velocity components and local energy dissipation in a stirred vessel generated by two propellers settled for various viscosities. Alcamo et al. [7] used smagorinsky model in the large-eddy simulation (LES) to model the unresolved, or sub-grid, scales to compute the turbulent flow field generated in an un-baffled stirred tank by a Rushton turbine. Gabriele et al. [8] used angle resolved particle image velocimetry to analyze the turbulent flow characteristics of an up-pumping pitched blade turbines and to be compared with their down-pumping equivalent. Otherwise, Driss et al. [9] studied the seeding particle mass quantity effect in the PIV measurement in a stirred vessel equipped by a Rushton turbine. Driss et al. [10] used 2D PIV technique to study the turbulent flow inside a cylindrical baffled stirred vessel with a set of speed ranging from 100 rpm to 350 rpm. Hassan et al. [11] used experimental apparatus to characterize an un-baffled vessel equipped with four nozzle spargers generated with anchor turbine in terms of power consumption and gas-liquid mass transfer. Huchet et al. [12] used experimental estimation of the dissipation rate of kinetic energy by means of time-resolved 2D-PIV, in the impeller region of a stirred vessel. Escudié and Liné [13] used two-dimensional PIV technique to analyze the different types of hydrodynamics motion coexist in the tank generated by a Rushton turbine. Datta et al. [14] used the pixel by pixel correlation method for consecutive frames in a given sensor plane to estimate particulate velocity components. Cameron [15] studied the accuracy, the resolution and the limitation of PIV algorithm in an open channel flow. Nguyen et al. [16] investigated the accuracy of the stereo particle image velocimetry in the boundary position. Gilo and Kääb [17] evaluated the performance of two different approaches to achieve sub-pixel precision of normalized cross-correlation. Boillot et al. [18] presented a process to estimate the time separated two successive laser pulses. Nasibov et al. [19] utilized enhancement approach using ROI option of imaging camera sensors to improve the performance of digital particle

image velocimetry (DPIV) systems. Pfadler et al. [20] validated the sub grid scale (SGS) models for large-eddy simulations (LES) of turbulent premixed flames experimental validation by PIV experience. Shi et al. [21] proposed multi-grid and iterative image deformation cross-correlations to improve two widely used particle-image velocimetry (PIV) algorithms with time-resolved PIV data-processing. Hinsch et al. [22] discussed the autocorrelation function for a large area interrogation in a PIV technique. Weng et al. [23] linked the central difference particle image pattern matching and image distortion analysis to resolve flow fields from coarsest grid to super-resolution grid. Shah et al. [24] studied two different interrogation areas and overlaps effect on the PIV images process.

Therefore, the aim of this research is to optimize the fundamental knowledge of the hydrodynamic structure in a stirred vessel generated by a height concave blades turbine.

2. Experiments Apparatus

Figure 1 shows the cylindrical vessel mounted in a squared vessel which filled by water. The height of the water is equal to the tank diameter (D=300 mm). The turbine diameter is equal to the half of the vessel diameter (d=D/2) and placed in the middle of the tank. Four equally spaced baffles which are placed in 90° from one another were used. Using the particle image velocimetry (PIV), the flow is illuminated by a Nd-YAG 532 nm pulsed laser source. The acquisition of the tow-dimensional images data was taken with a CCD camera with 1600 x 1200 pixels² of resolution. The results were obtained for 170 images. The diameter of the seeding particle was equal to d_p=20 µm with 0.15 g of concentration [25-27].

Fig. 1. *Stirred tank equipped by a concave blades turbine.*

3. Experimental Results

In this study, The Reynolds number is equal to Re=26250. In addition, three azimuthally planes were investigated which present the turbine blade plane (θ=30°), the plane in the upstream of the turbine blade (θ=10°) and the plane in the downstream of the turbine blade plane (θ=45°).

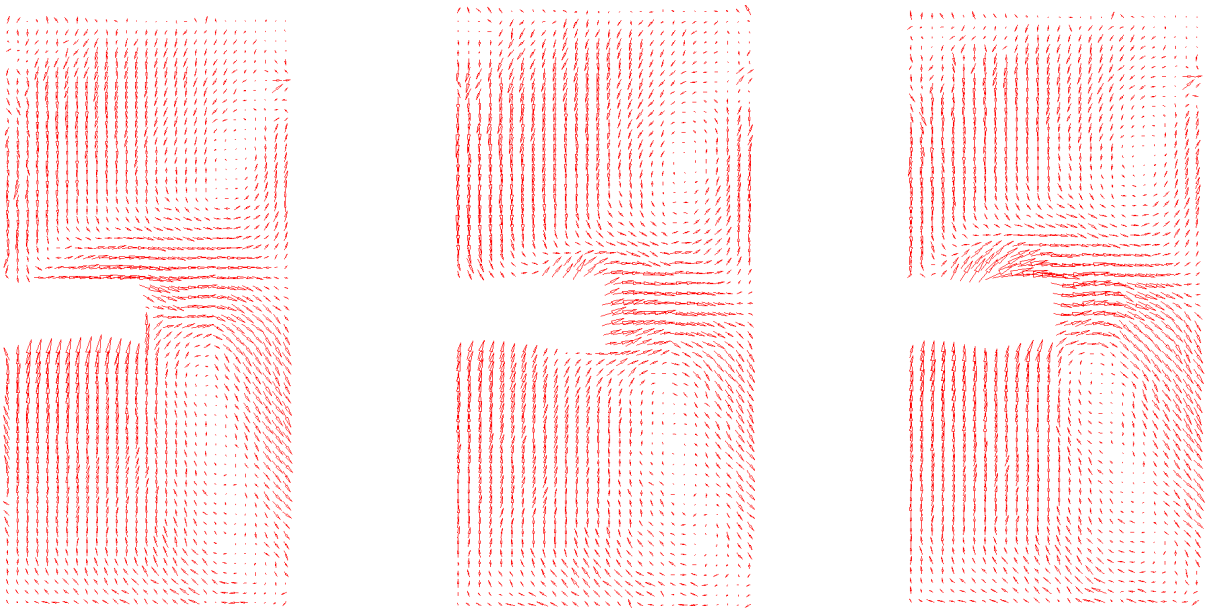

(a) θ=10° (b) θ=30° (c) θ=45°

Fig. 2. *Velocity fields.*

3.1. Velocity Fields

Figure 2 shows the velocity fields of the concave blades turbine. In fact, we present three different planes θ=10°, θ=30° and θ=45°. According to these results, two recirculation loops were observed. The first one is localized in the upper region of the tank near the free surface. However, the second one is localized in the bottom of the tank which is the largest. At the blade end, the velocity is almost radial with some deviation for all configurations. In addition, in the blade plane defined by θ=30° and in the downstream plane blade defined by θ=45°, a vertical velocity has been observed upper the blade. Afterward, near the wall of the vessel, the velocity is divided into the upward and downward flow. Indeed, the lowest mean velocity has been observed in the blade plane defined by θ=30°, where the velocity value is equal to V_m=28.8 mm/s. In the other planes, the mean velocity is almost the same.

3.2. Fluctuating Velocity

Figure 3 shows the normalized RMS velocity distribution of the concave blades turbine. Three different planes defined by θ=10°, θ=30° and θ=45° were presented. According to these results, the lowest values areas are localized in the center of the circulation loop which described with lowest velocity. Otherwise, the high value areas are spreader in the bulk region of the tank. Therefore, they are found in the same direction of the discharge flow. Obviously, the highest values areas are localized around the blade, near the vessel wall and near the shaft. In addition, the highest normalized RMS value is presented in the downstream plane blade defined by θ=45°.

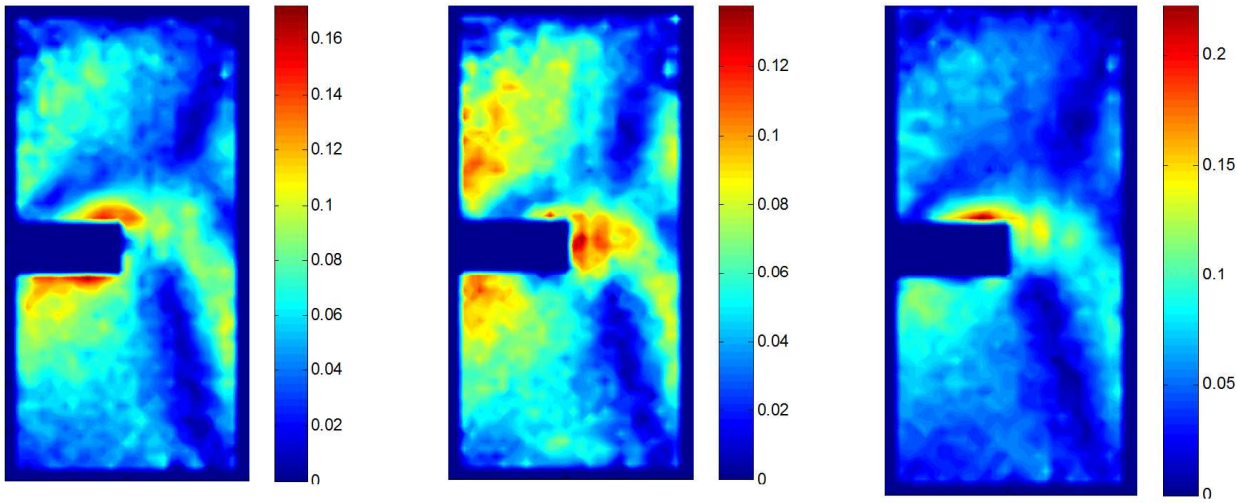

(a) θ=10° (b) θ=30° (c) θ=45°

Fig. 3. *Distribution of the mean normalized RMS.*

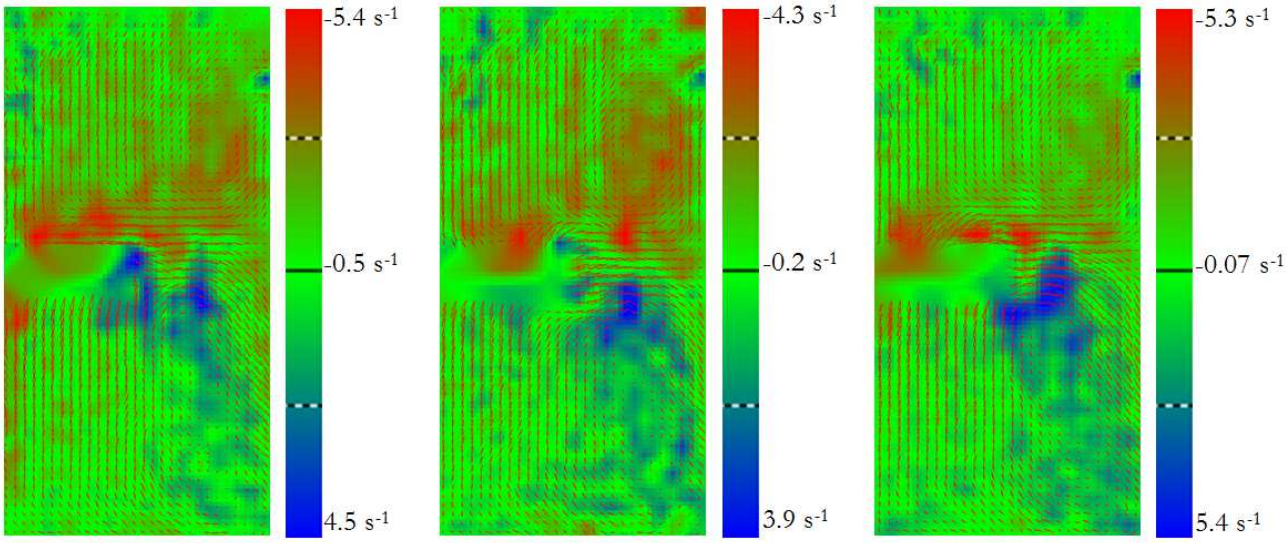

(a) θ=10° (b) θ=30° (c) θ=45°

Fig. 4. *Distribution of the vorticity.*

3.3. Vorticity

Figure 4 shows the vorticity distribution generated with the concave blades turbine. In this study, we compare the vorticity distribution in three different planes defined by θ=10°, θ=30° and θ=45°. According to these results, the bulk region of the tank is presented with the medium vorticity value. Moreover, the highest value area is localized in the upper region of the tank which follows the same direction of the first circulation loop. In addition, the highest value area is also localized in the above of the blade. Thereby, the lowest value area is localized in the inferior region of the tank which follows the same direction of the second circulation loop. The plane in the downstream of the blade plane (θ=45°) is described with the highest vorticity values.

3.4. Turbulent Kinetic Energy

Figure 5 shows the distribution of the turbulent kinetic energy of the concave blades turbine. In this study, we compare the results in three different planes defined by θ=10°, θ=30° and θ=45°. According to these results, the turbulent kinetic energy presents his maximum at the blade region and decreases progressively moving away from the blade. Furthermore, for the angular position equal to θ=45°, the maximum region is localized above the blade with the same direction of the circulation loop.

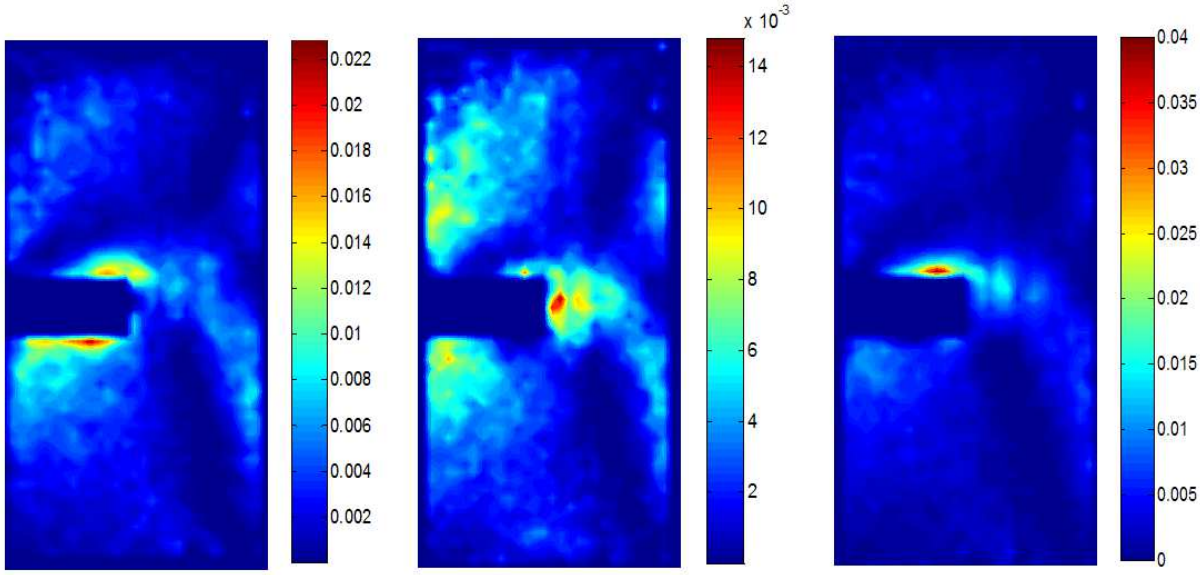

Fig. 5. *Distribution of the turbulent kinetic energy.*

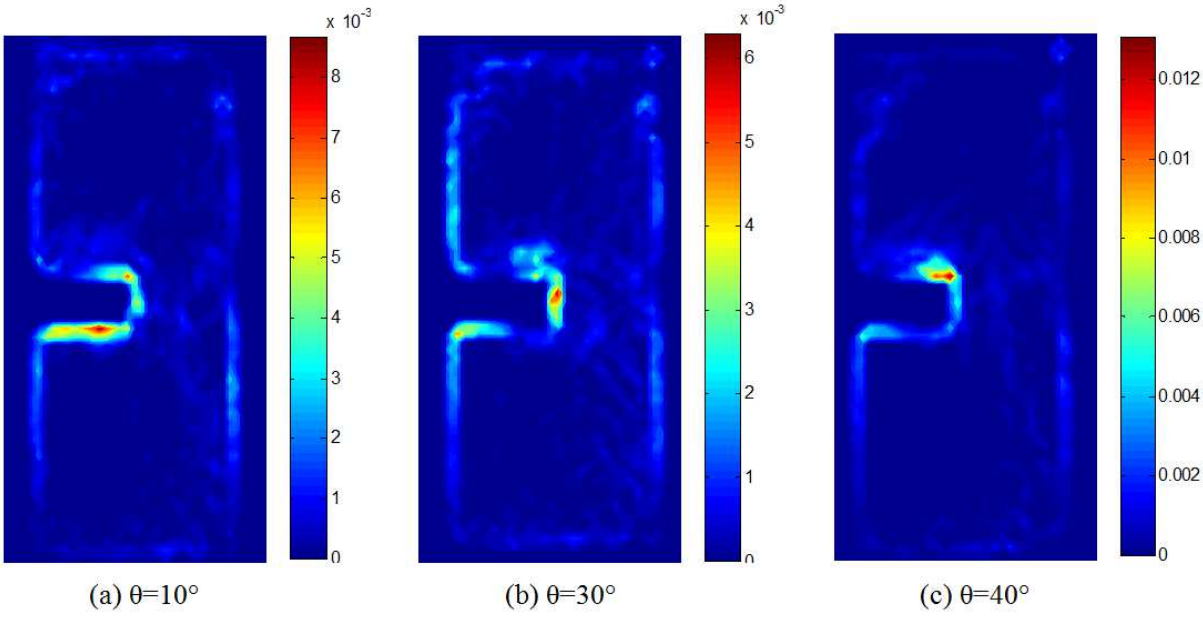

Fig. 6. *Distribution of the dissipation rate of the turbulent kinetic energy.*

3.5. Dissipation Rate of the Turbulent Kinetic Energy

Figure 6 shows the distribution of the dissipation rate of the turbulent kinetic energy of the concave blades turbine. Three different presentation planes θ=10°, θ=30° and θ=45° were considered. According to these results, the dissipation rate of the turbulent kinetic energy presents his maximum near the blade region and decreases progressively moving away from the blade. Furthermore, for the angular position equal to θ=10° and θ=45°, other maximum region were found which localized around the blade.

3.6. Turbulent Viscosity

Figure 7 shows the distribution of the turbulent viscosity of the concave blades turbine. Three different presentation planes θ=10°, θ=30° and θ=45° were considered. According to these results, the turbulent viscosity presents his maximum near the blade region and decreases progressively moving away from the blade. Obviously, the highest value area is localized under the blade for the angular position equal to θ=10°. However, the highest value area is localized above the blade for the angular position equal to θ=45°.

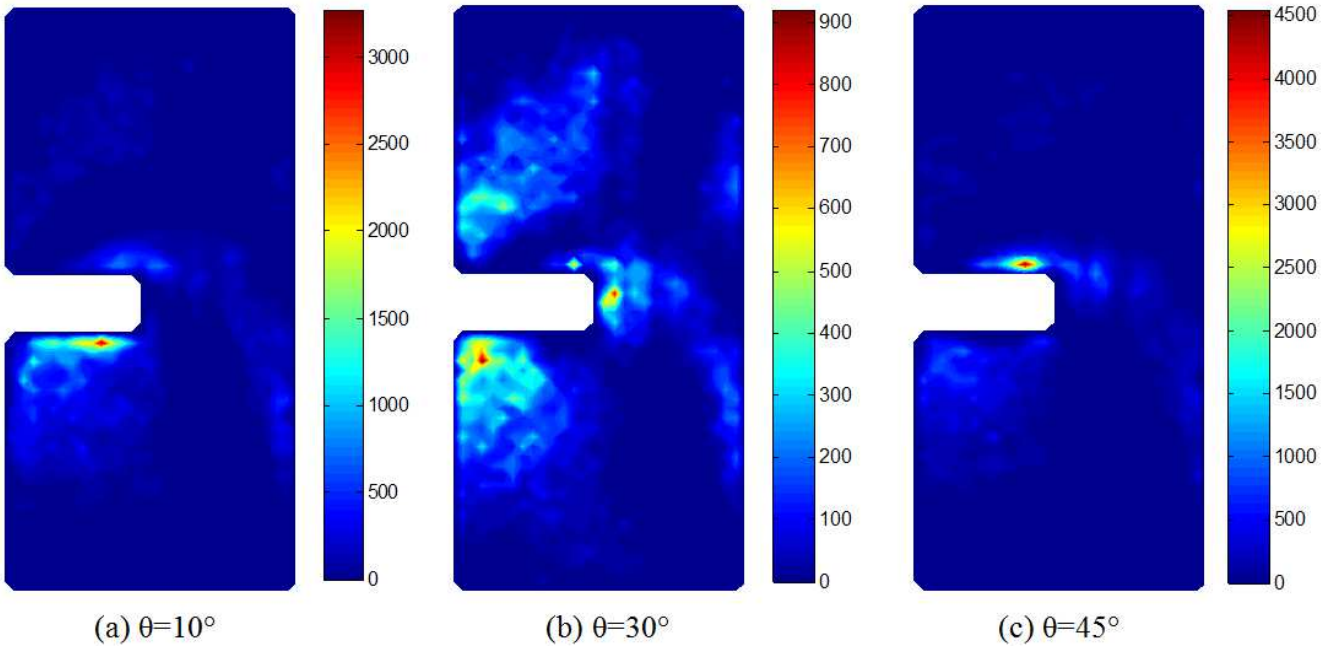

Fig. 7. *Distribution of the turbulent viscosity.*

4. Conclusion

In this paper, an experimental investigation of the concave blades turbine was carried out. In fact, three different planes θ=10°, θ=30° and θ=45° have been considered. Several results were presented which describe the velocity field, the vorticity, the turbulent kinetic energy, the dissipation rate of the turbulent kinetic energy and the turbulent viscosity. Particularly, it has been observed that the velocity has the some deviation above the blade region compared to the previous works. Indeed, it is essential to note that the concave blades turbine can improve the stirring operation in the vessels tanks.

References

[1] Driss Z., Karray S., Kchaou H., Abid M. S., 2011, CFD simulation of the laminar flow in stirred tanks generated by double helical ribbons and double helical screw ribbons impellers, Cent. Eur. J. Eng., 1(4), 413-422.

[2] Chtourou W., Ammar M., Driss Z., Abid M. S., 2011, Effect of the turbulence models on Rushton turbine generated flow in a stirred vessel, Cent. Eur. J. Eng., 1(4), 380-389.

[3] Bouzgarrou G., Driss Z., Abid M. S., 2009, Etude de la structure hydrodynamique dans une cuve agitée générée par des hélices, Récents Progrès en Génie des Procédés, 98.

[4] Driss Z., Kchaou H., Baccar M., Abid M. S., 2005, Numerical investigation of internal laminar flow generated by a retreated-blade paddle and a flat-blade paddle in a vessel tank, Int. J. Eng. Simul., 6, 10-16.

[5] Karray S., Driss Z., Kchaou H., Abid M. S., 2011, Hydromechanics characterization of the turbulent flow generated by anchor impellers, Engeneering Applications of Computational Fluid Mechanics, 5 (3), 315-328.

[6] Xuereb C., Bertrand J., 1996, 3-D hydrodynamics in a tank stirred by a double-propeller system and filled with a liquid having evolving rheological properties, Chemical Engineering Science, 51 (10), 1725-1734.

[7] Alcamo R., Micale G., Grisafi F., Brucato A., Ciofalo M., 2005, Large-eddy simulation of turbulent flowin an unbaffled stirred tank driven by a Rushton turbine, Chemical Engineering Science, 60, 2303-2316.

[8] Gabriele A., Nienow A.W., Simmons M.J.H., 2009, Use of angle resolved PIV to estimate local specific energy dissipation rates for up- and down-pumping pitched blade agitators in a stirred tank, Chemical Engineering Science, 64, 126-143.

[9] Driss Z., Bouzgarrou G., Kaffel A., Chtourou W., Abid M. S., 2012, Experimental Study of the Seeding Mass Quantity Effect on the PIV Measurements Applied on a Stirred Vessel Equipped by a Rushton Turbine, International Journal of Mechanics and Applications, 2(5), 93-97.

[10] Driss Z., Ahmed K., Bilel B. A., Ghazi B., Mohamed S. A., 2012, PIV measurements to study the effect of the Reynolds number on the hydrodynamic structure in a baffled vessel stirred by a Rushton turbine, Science Academy Transactions on Renewable Energy Systems Engineering and Technology, 2 (4), 2046–6404.

[11] Hassan R., Loubiere K., Legrand J., 2009, Power consumption and mass transfer in an un-baffled stirred tank for autothermal thermophilic digestion of sludge, Récents Progrès en Génie des Procédés, 98.

[12] Huchet F., Liné A., Morchain J., 2009, Evaluation of local kinetic energy dissipation rate in the impeller stream of a Rushton turbine by time-resolved PIV, Chemical Engineering Research and Design, 8, 369-376.

[13] Escudié R., Liné A., 2003, Experimental Analysis of Hydrodynamics in a Radially Agitated Tank, AIChE Journal, 49(3), 585-603.

[14] Datta U., Dyakowski T., Mylvaganam S., 2007, Estimation of particulate velocity components in pneumatic transport using pixel based correlation with dual plane ECT, Chemical Engineering Journal, 130, 87-99.

[15] Cameron S. M., 2011, PIV algorithms for open-channel turbulence research: Accuracy, resolution and limitations, Journal of Hydro-environment Research, 5, 247-262.

[16] Nguyen T. D., Wells J. C., Nguyen C. V., 2010, Wall shear stress measurement of near-wall flow over inclined and curved boundaries by stereo interfacial particle image velocimetry, International Journal of Heat and Fluid Flow, 31, 442-449.

[17] Gilo M. D. And Kääb A., 2011, Sub-pixel precision image matching for measuring surface displacements on mass movements using normalized cross-correlation, Remote Sensing of Environment 115, 130-142.

[18] Boillot A., Prasad A.K., 1996, Optimization procedure for pulse separation in cross-correlation PIV, Experiments in Fluids, 21, 87-93.

[19] Nasibov H., Kholmatov A., Kselli B., Nasibov A., 2012, A PIV dynamic velocity range enhancement approach using ROI option of imaging sensors, Flow Measurement and Instrumentation, 28, 35-44.

[20] Pfadler S., Dinkelacker F., Beyrau F., Leipertz A., 2009, High resolution dual-plane stereo-PIV for validation of sub grid scale models in large-eddy simulations of turbulent premixed flames, Combustion and Flame, 156, 1552-1564.

[21] Shi S., New T.H., Liu Y., 2013, Improvements to time-series TR-PIV algorithms using historical displacement and displacement variation information, Flow Measurement and Instrumentation, 29, 67-79.

[22] Hinsch K., Arnold W., Platen W., 1988, Flow Field Analysis by Large-Area Interrogation in Particle Image Velocimetry, Optics and Lasers Engineering, 9, 229-243.

[23] Weng W., Jaw S., Chen J., Hwang R. R., Optimization of particle image distortion for PIV measurements, 9th International Conference on Hydrodynamics October, 11-15, 2010, Shanghai, China.

[24] Shah M.K., Agelinchaab M., Tachie M.F., 2008, Influence of PIV interrogation area on turbulent statistics up to 4th order moments in smooth and rough wall turbulent flows, Experimental Thermal and Fluid Science, 32, 725-747.

[25] Driss Z., Kaffel A., Ben Amira B., Bouzgarrou G., Abid M. S., PIV measurements to study the effect of the Reynolds number on the hydrodynamic structure in a baffled vessel stirred by a Rushton turbine, American Journal of Energy Research, 2 (3), 67-73, 2014.

[26] Ben Amira B., Driss Z., Abid M. S., PIV Study of the Interrogation Area Size Effect on the Hydrodynamic Results of a Stirred Vessel Equipped by an Eight Flat Blades Turbine. International Journal of Fluid Mechanics & Thermal Sciences, 1(3), 42-48, 2015.

[27] Ben Amira B., Driss Z., Abid M.S., 2015, Experimental study of the up-pitching blade effect with a PIV application, Ocean Engineering, 102, 95-104.